



**HAL**  
open science

## Near-Infrared and Visible Dual-Emitting Peptide by Modular Assembly of Nitrobenzoxadiazole and Neodymium Complexes

Yik-hoi Yeung, Ho-fai Chau, Hei-yui Kai, Wanqi Zhou, Kaitlin Hao-yi Chan, Waygen Thor, Loïc Charbonnière, Fan Zhang, Yong Fan, Yue Wu, et al.

► **To cite this version:**

Yik-hoi Yeung, Ho-fai Chau, Hei-yui Kai, Wanqi Zhou, Kaitlin Hao-yi Chan, et al.. Near-Infrared and Visible Dual-Emitting Peptide by Modular Assembly of Nitrobenzoxadiazole and Neodymium Complexes. *Advanced Optical Materials*, 2024, 12 (9), pp.2302070. 10.1002/adom.202302070 . hal-04750052

**HAL Id: hal-04750052**

**<https://hal.science/hal-04750052v1>**

Submitted on 5 Nov 2024

**HAL** is a multi-disciplinary open access archive for the deposit and dissemination of scientific research documents, whether they are published or not. The documents may come from teaching and research institutions in France or abroad, or from public or private research centers.

L'archive ouverte pluridisciplinaire **HAL**, est destinée au dépôt et à la diffusion de documents scientifiques de niveau recherche, publiés ou non, émanant des établissements d'enseignement et de recherche français ou étrangers, des laboratoires publics ou privés.

# Near-Infrared and Visible Dual-Emitting Peptide by Modular Assembly of Nitrobenzoxadiazole and Neodymium Complexes

Yik-Hoi Yeung, Ho-Fai Chau, Hei-Yui Kai, Wanqi Zhou, Kaitlin Hao-Yi Chan, Waygen Thor, Loïc J. Charbonnière, Fan Zhang, Yong Fan, Yue Wu,\* and Ka-Leung Wong\*

The synthetic difficulty of target-specific lanthanide complexes, despite their unique characteristics, limits their use in *in vitro*/ *in vivo* studies and biomedical applications. With commercially available and affordable reagents, a facile synthetic approach is developed to modularly deploy nitrobenzoxadiazole and neodymium complexes onto bioactive peptides. The yielded probes show observable neodymium emission with specific localization to corresponding biotargets *in vitro*, which became the first example of a stable, water-soluble, and target-specific neodymium(III) complex applicable for *in vitro* imaging with detectable brightness.

## 1. Introduction

As an advanced non-invasive imaging technique with less background interference, deeper tissue penetration, and higher signal-to-noise ratio and imaging resolution, near-infrared (NIR, 700–1700 nm) imaging has received considerable research interest and has been used in clinical applications (e.g., real-time visualization in diagnosis and surgical operations) in

recent decades.<sup>[1–5]</sup> A variety of organic NIR dyes have been developed,<sup>[6,7]</sup> but they showed several drawbacks such as photobleaching in physiological conditions, small Stokes shift, and high toxicity.<sup>[8]</sup> Lanthanide complexes are regarded as promising alternatives due to their high photostability, large ligand-induced Stokes shift, and relatively long luminescent lifetimes that enable the time-gated imaging technique.<sup>[9,10]</sup> Yb<sup>3+</sup> and Er<sup>3+</sup> have been used for both *in vitro* and *in vivo* imaging<sup>[2,3,8]</sup> but no Nd<sup>3+</sup> complexes have been developed as an *in vitro* imaging probe<sup>[11–13]</sup> due to their low

luminescent quantum yield, which is attributed to the convoluted energy states and severe vibration of Nd<sup>3+</sup> complex.<sup>[14]</sup> Nevertheless, we still consider the distinct NIR emission pattern of Nd<sup>3+</sup> complexes, especially its emission bands in NIR-II windows (<sup>4</sup>F<sub>3/2</sub> → <sup>4</sup>I<sub>11/2</sub>, 1060 nm, <sup>4</sup>F<sub>3/2</sub> → <sup>4</sup>I<sub>13/2</sub>, ≈1330 nm) valuable for the development of NIR probes as this emission range is applicable in commercially available hardware set-ups of confocal microscopy, rendering practical applications rather than having to wait for hardware development to catch up with the properties of the probes.

Peptide-based drugs are gaining much research interest in recent decades as they are regarded as promising modulators for large and shallow binding interface of protein-protein interactions (PPIs) while solid-phase peptide synthesis (SPPS) provides a platform to assemble peptides from a rich commercial sources of amino acid building blocks. Nitrobenzoxadiazoles (NBD) is a family of small fluorescent dyes commonly utilized for imaging and sensing.<sup>[15,16]</sup> NBD conjugated on primary amines (including N-terminal or lysine side chain of peptides) are stable and sensitive to the environment and thus are being employed in targeted imaging,<sup>[17]</sup> monitoring of self-assemble peptide,<sup>[18]</sup> etc. Recently, Sénèque et al. developed a zinc sensor based on the distal energy transfer between NBD and Nd-DO3A (the complex of Nd<sup>3+</sup> and cyclen based-chelator 1,4,7,10-tetraazacyclododecane-1,4,7-triacetic acid), while upon conformational change of the peptide over zinc coordination, the luminescent intensity was enhanced.<sup>[19]</sup> Target-specific luminescent lanthanide complexes are usually composed of a lanthanide complex, a targeting motif, as well as an antenna that transfer energy from external light to lanthanide ion.<sup>[13,20–24]</sup> In previous studies, antenna or lanthanide complex has to be a bifunctional motif that can bridge other two components, such molecules are usually accompanied

Y.-H. Yeung, H.-F. Chau, H.-Y. Kai, Y. Wu, K.-L. Wong  
Department of Applied Biology and Chemical Technology  
The Hong Kong Polytechnic University  
11 Yuk Choi Rd Hung Hom, Hong Kong, SAR China  
E-mail: [yue\\_wu@life.hkbu.edu.hk](mailto:yue_wu@life.hkbu.edu.hk); [klgwong@polyu.edu.hk](mailto:klgwong@polyu.edu.hk)

Y.-H. Yeung, H.-Y. Kai, W. Zhou, K. H.-Y. Chan, W. Thor, Y. Wu  
Department of Chemistry  
Hong Kong Baptist University  
224 Waterloo Rd, Kowloon Tong Kowloon, Hong Kong, SAR China  
W. Thor, L. J. Charbonnière  
Equipe de synthèse pour l'analyse (SynPA)  
Institut Pluridisciplinaire Hubert Curien (IPHC)  
Département des sciences analytiques (DSA) – UMR 7178  
CNRS/Université de Strasbourg  
ECPM  
Bâtiment R1N0, 25, rue Becquerel, Cedex-2, Strasbourg 67087, France

F. Zhang, Y. Fan  
Department of Chemistry  
State Key Laboratory of Molecular Engineering of Polymers and iChem  
Shanghai Key Laboratory of Molecular Catalysis and Innovative Materials  
Fudan University  
2005 Songhu Road, Yangpu, Shanghai 200438, China

The ORCID identification number(s) for the author(s) of this article can be found under <https://doi.org/10.1002/adom.202302070>

DOI: 10.1002/adom.202302070

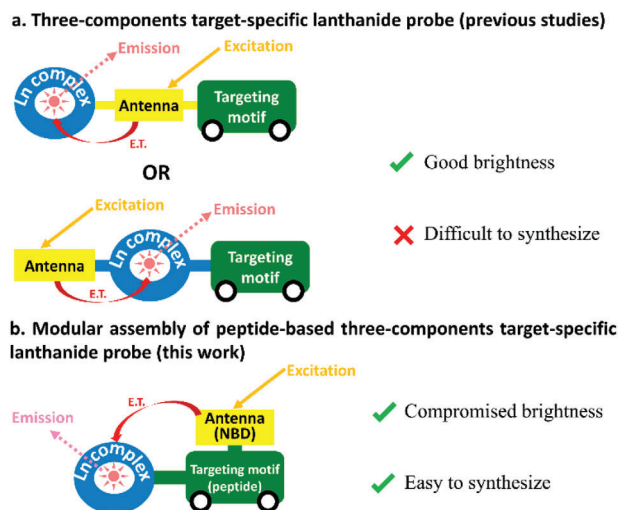


**Figure 1.** Strategies in synthesizing target-specific lanthanide complexes. a) Presynthesized bifunctional antenna/chelator linked to targeting motif to exhibit direct energy transfer; b) Modular installation of antenna and chelator on branched peptide to exhibit distal energy transfer.

with significant synthetic difficulties (Figure 1a). Inspired by S n que et al., we considered using target-specific peptides with orthogonally protected amino acid as a bifunctional framework to construct such three-components lanthanide-based bioprobes. By strategical deprotections of the orthogonally protected amino acid, NBD and Nd-DO<sub>3</sub>A can be sequentially assembled onto the  $\alpha$ -amine and side chain of the peptide respectively to yield a visible and NIR dual-emitting probe (Figure 1b).

## 2. Results and Discussion

Although most of the previous studies used NBD-functionalized amino acid building blocks [e.g., NBD-Gly-OH, NBD- $\beta$ -Ala-OH or Fmoc-Dap(NBD)-OH] to label peptides with NBD, we considered direct introduction of commercially available 4-chloro-7-nitrobenzofurazan (NBD-Cl) with primary amine on peptide to achieve modular assembly (Figure 2a). Incubation of NBD-Cl and DIPEA with resin-bound YRGD peptide gave a maximum of 92% conversion after 24 h reaction (Figure 2b) while multiple couplings gave a maximum of 96% conversion (Figure 2c). Surprisingly, GYRGD or XYGRD, spaced by Gly (G, glycine) or Ahx (6-aminohexanoic acid, abbreviated as X in this manuscript) from the bulky side chain of Tyr, were consumed completely (Figure 2d). To further verify the influence of steric effects, reactions were also conducted on endoplasmic reticulum (ER)-targeting peptide XWEKDEL and WEKDEL.<sup>[25]</sup> As a result, XWEKDEL was fully converted into the corresponding NBD conjugate, while only 63% conversion was achieved by WEKDEL, correlating with the steric effect from large indole side chain of Trp (Figure 2e,f). The reaction performed on mitochondria-targeting peptide XYKLAKLAKLAKLAK (16-mers) derived from previous studies<sup>[26–28]</sup> gave a complete conversion, suggesting that steric effect was more significant than peptide length in terms of NBD conjugation (Figure 2g). To compare the isolated yield of products synthesized from direct coupling and building block approach, NBD-functionalized Ahx building block, NBD-Ahx-OH, was cou-

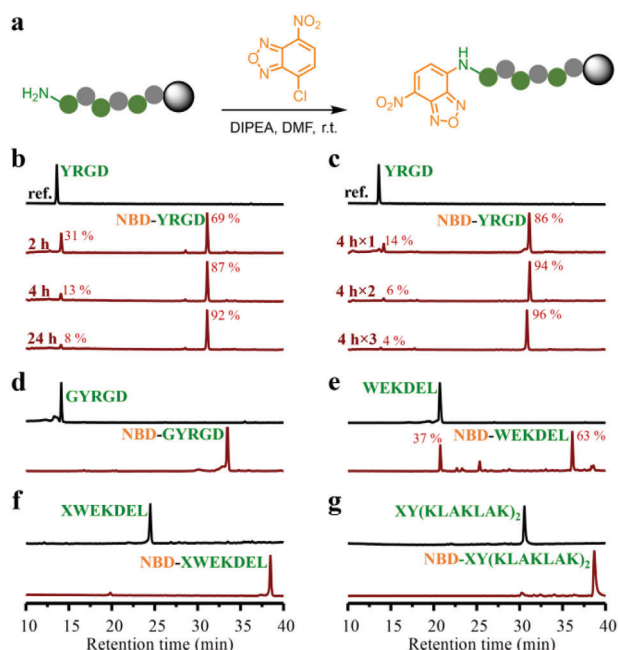


**Figure 2.** Trials of direct incorporation of NBD on the N-terminal of resin-bound peptides, reacted for 4 h unless specified; % conversion are defined as the peak area of desired product over the sum of peak area of desired product and starting peptide, calc. based on abs. at 280 nm from the chromatogram. a) General approach to incorporate NBD on peptide by incubating the solution of NBD-Cl and DIPEA in DMF; b) Trials of different reaction time on YRGD peptide; c) Trials of different times of reaction on YRGD peptide; d) Trials of direct incorporation of NBD on resin-bound peptide with non-bulky spacer; e, f) Comparison of direct incorporation of NBD on WEKDEL and XWEKDEL, respectively; g) Comparison of introducing NBD with NBD-X building block and direct incorporation on (KLAKLAK)<sub>2</sub>.

pled to WEKDEL and YKLAKLAKLAKLAK peptides. As a result, the isolated yields from our direct coupling approach and traditional building block approach are found comparable (79% and 80% for WEKDEL, 42% and 43% for YKLAKLAKLAKLAK respectively). We therefore concluded that the direct reaction between NBD-Cl and the non-bulky amine group on peptide is effective and comparable to the building block approach used in most of previous studies.<sup>[17,18]</sup>

We then conducted modular construction of NIR and visible dual-emitting peptide (Figure 3a). Two orthogonally protected amino acids, Fmoc-Dap(Mtt)-OH (with one side chain -CH<sub>2</sub>-) and Fmoc-Lys(Mtt)-OH (with four side chain -CH<sub>2</sub>-), were chosen as an extension hub to accommodate NBD and DO<sub>3</sub>A, where the difference in side chain length helps compare the relations between antenna-complex distance and energy transfer efficiency. The orthogonally protected amino acids were incorporated onto resin-bound RGD peptide first. With regards to the above-mentioned steric effect, direct installation of NBD was hence conducted on the relatively non-bulky side chain amine instead of  $\alpha$ -amine. The protecting group on the side chain, Mtt, was strategically removed to accommodate NBD-Cl. The Fmoc protecting group on N-terminal was then removed, and the DO<sub>3</sub>A-motif was further incorporated by an established two-step solid-phase approach with commercially available and af-

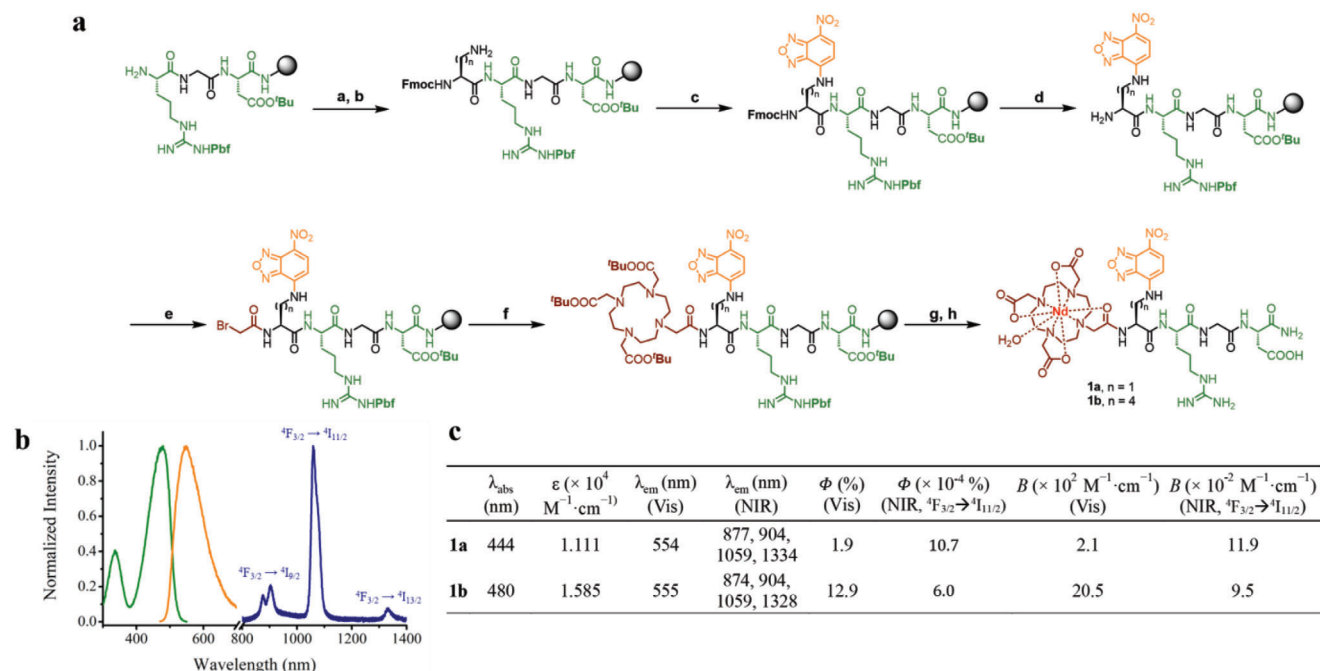


**Figure 3.** a) Modular synthetic route for constructing dual Vis/NIR emitting probe on RGD peptide. Reagents and conditions: a. Installation of extension hub. Fmoc-Lys/Dap(Mtt)-OH, PyBOP, DIPEA, DMF, 2–16 h; b) Mtt deprotection. 1% TFA and 1% TIPS in DCM (v/v), 2 min  $\times$  5; c) Installation of antenna. NBD-Cl, DIPEA, DMF, 16 h; d) Fmoc deprotection. 20% 4-methylpiperidine in DMF (v/v), 25 min; e) Installation of brancher. BrCH<sub>2</sub>COOH, DIC, DMF, 1 h; f) Installation of chelator. tri-<sup>t</sup>Bu-DO3A, DIPEA, DMF, 16 h; g) Global cleavage and deprotection, 95% TFA, 2.5% TIPS, 2.5% H<sub>2</sub>O; h) Nd chelation. NdCl<sub>3</sub>·6H<sub>2</sub>O, pH 7.4, 16 h; (b) Normalized excitation (green) and emission (orange for visible, navy for NIR) spectra of 1a. (c) Summary of photophysical properties of 1a and 1b.

fordable building blocks (bromoacetic acid and tri-<sup>t</sup>Bu-DO3A).<sup>[29]</sup> The Nd<sup>3+</sup> was finally chelated after global cleavage and deprotection to give the desired product **1a** and **1b**, where Dap and Lys serve as an extension hub to link a Nd complex and an antenna together, respectively. Completeness of conversion was monitored by HPLC and ESI-MS step-by-step (Figure S1, Supporting Information), and the isolated yield of **1a** and **1b** reached 21% and 22%, respectively. These results show the high efficiency of our modular synthetic approach for desired bifunctionalized peptides.

By measuring the photophysical properties of **1a** and **1b**, the green-to-yellow fluorescence (maxima at  $\approx$ 555 nm) from NBD motif and three characteristic NIR emission bands of Nd luminescence ( ${}^4\text{F}_{3/2} \rightarrow {}^4\text{I}_{9/2}$ , two peaks at  $\sim$ 875 nm, 904 nm;  ${}^4\text{F}_{3/2} \rightarrow {}^4\text{I}_{11/2}$ , 1059 nm,  ${}^4\text{F}_{3/2} \rightarrow {}^4\text{I}_{13/2}$ ,  $\sim$ 1330 nm) could be identified for both compounds (Figure 3b). The luminescent quantum yields of **1a** and **1b** were determined to be  $1.1 \times 10^{-3}\%$  and  $6.0 \times 10^{-4}\%$ , respectively, both slightly higher than the NIR-emitting Nd<sup>3+</sup> complex reported by S en eque et al. ( $5.0 \times 10^{-4}\%$ , without Zn<sup>2+</sup>). However, considering the application of bioimaging, the term “brightness” can better quantify the signal intensity for detection rather than quantum yield. We therefore calculated the brightness of **1a** and **1b** by our previously reported definition<sup>[30,31]</sup> with the following equation:

$$B = \Phi(\lambda) \times \epsilon(\lambda) \quad (1)$$

where brightness (unit =  $\text{M}^{-1} \text{cm}^{-1}$ ) is defined as the product of quantum yield and molar absorptivity of a compound under certain wavelength. The NIR brightness of compounds **1a** and **1b**

for the  ${}^4\text{F}_{3/2} \rightarrow {}^4\text{I}_{11/2}$  transition (1059 nm) were found to be 0.119 and  $0.095 \text{M}^{-1} \text{cm}^{-1}$  (Figure 3c). As expected, **1a** showed a higher NIR quantum yield and brightness than **1b** due to the relatively shorter distance between its Nd<sup>3+</sup> complex and antenna. Nevertheless, in view of the relatively high cost of unnatural amino acid Dap (as well as Dab and Orn) with orthogonal protections, orthogonally protected proteinogenic amino acid Lys can be compromised as an ideal extension hub giving significant visible and NIR brightness at low cost.

We further applied this approach on a series of relatively long resin-bound peptides, such as nucleus localization sequence (NLS, PKKKRKV, 7-mers, to synthesize desired compound **2**), mitochondria localization sequence [MLS, (KLAKLAK)<sub>2</sub>, 14-mers, to synthesize desired compound **3**], as well as Epstein-Barr virus nuclear antigen 1 (EBNA1)-targeting peptide that we previously reported (XYFMVFGGRrRK, 12-mers, to synthesize desired product **4**).<sup>[32–34]</sup> All these trials gave satisfactory conversion (74% for **2**, 56% for **3** and 61% for **4**) and isolated yields (27% for **2**, 12% for **3**, and 45% for **4**) (Figure 4a), which indicates that our protocol is versatile for various bioactive peptides on resin. All synthesized products showed similar photophysical properties with compound **1b** because they share identical chromophores, their photophysical data have been summarized in Table S5 (Supporting Information).

To demonstrate the potential application of synthesized compounds as target-specific near-infrared and visible dual-emitting luminescent probes, compounds **3** and **4** were chosen as model studies of in vitro cell imaging experiments. As expected, both visible and NIR emissions from compound **3** well co-localized



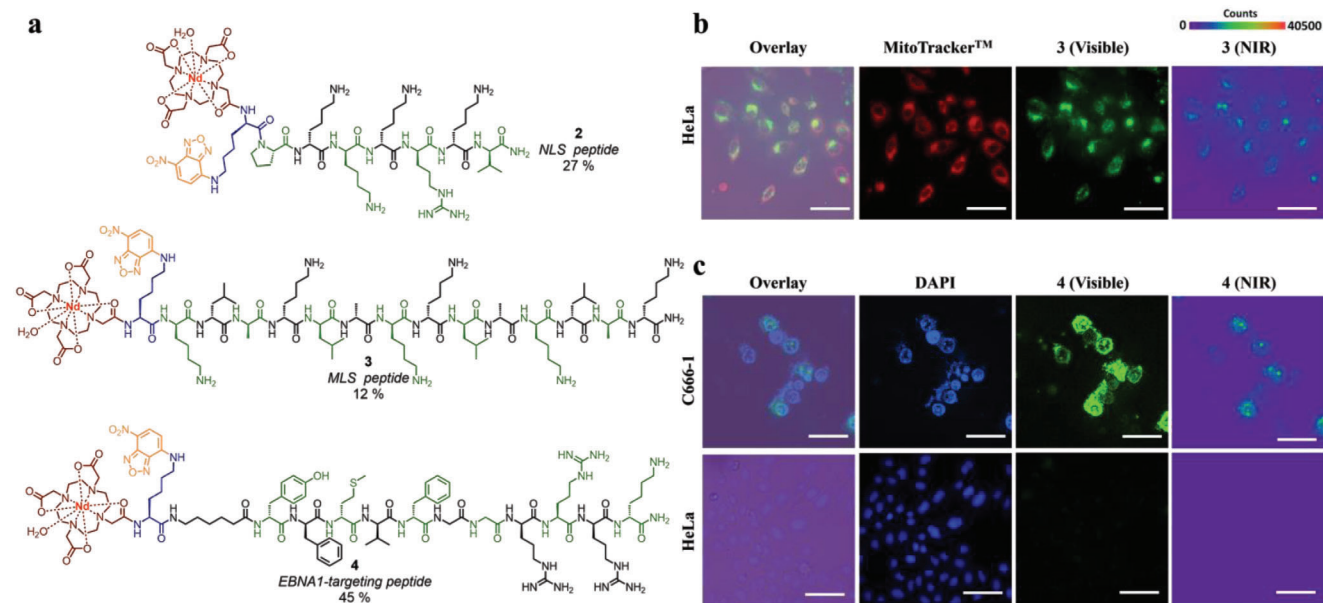


**Figure 4.** a) Structure of synthesized compound 2, 3 and 4; b) Cellular imaging of HeLa co-stained with MitoTracker Red (mitochondria staining dye with red fluorescence) after incubation of compound 3 (derived from mitochondria targeting peptide) for 24 h (scale bar: 25  $\mu$ m), Pearson's coefficient:  $r = 0.684$ ; c) Cellular imaging of C666-1 (EBNA+) and HeLa (EBNA-) co-stained with DAPI (nucleus staining dye with blue fluorescence) after incubation of compound 4 (functionalized EBNA1 targeting peptide) for 24 h (scale bar: 25  $\mu$ m). For C666-1 cell line, Pearson's coefficient:  $r = 0.723$ .

with red fluorescence from MitoTracker Red ( $r = 0.684$ ) in the mitochondria of the HeLa cell line (Figure 4b). Moreover, compound 4 also displayed decent uptake in the nucleus of the EBNA1-positive C666-1 cell line with both visible and NIR signal ( $r = 0.723$ ) while it was merely detected in the EBNA1-negative HeLa cell line. These results showed the potential for compounds 3 & 4 synthesized from our modular synthetic approach as near-infrared and visible dual-emitting luminescent probes with target specificity inherent from their conjugated peptide. To the best of our knowledge, this is the first example of performing cellular imaging with targeting probes based on the NIR emission of  $\text{Nd}^{3+}$  complex.

### 3. Conclusion

In this work, we found that the reaction efficiency between NBD-Cl and amine on resin-bound peptide is very sensitive to the bulkiness of reaction site. By introducing a spacer or conducting the reaction on a non-bulky (e.g., side chain) amine purposely, direct incorporation of NBD can be conducted efficiently without using presynthesized NBD building blocks. Based on that, we further developed a modular synthetic approach to assemble an NIR and visible dual-emitting neodymium complex on peptide by functionalizing an orthogonally protected amino acid with NBD (visible emitter and antenna for  $\text{Nd}^{3+}$ ) on its side chain and DO3A (chelator for  $\text{Nd}^{3+}$ ) on its N-terminal, respectively. The desired products with NIR and visible dual-emission can be obtained with good yields by single-time HPLC purification after global cleavage and metal chelation, for various bioactive peptides. As a model study, we report the first stable and water-soluble  $\text{Nd}^{3+}$  complex-based imaging probe compound 4 that can differentiate EBNA1-positive and EBNA1-negative cell lines by both visi-

ble and NIR signals in in vitro cell imaging experiments, demonstrating the potential of newly reported synthetic approach in the preparation of luminescent bioprobes with detectable NIR emissions.

### Supporting Information

Supporting Information is available from the Wiley Online Library or from the author.

### Acknowledgements

K.-L.W. gratefully acknowledges the financial assistance from the Hong Kong Research Grants Council Grant No. 12300021, NSFC/RGC Joint Research Scheme (N\_PolyU209/21), and the Centre for Medical Engineering of Molecular and Biological Probes (AoE/M-401/20). The precious advice in writing provided by Dr. Wai-Sum Lo from the Department of Applied Biology and Chemical Technology (ABCT) of The Hong Kong Polytechnic University (HKPolyU) is greatly appreciated. The authors also appreciate the service of high-resolution mass spectrometry provided by The University Research Facility in Life Sciences (ULS) of HKPolyU.

### Conflict of Interest

The authors declare no conflict of interest.

### Data Availability Statement

The data that support the findings of this study are available in the supplementary material of this article.

### Keywords

lanthanide probes, neodymium, NIR probes, nitrobenzoxadiazole, solid-phase peptide synthesis

Received: August 29, 2023  
Revised: January 17, 2024  
Published online: February 10, 2024

- [1] G. Hong, A. L. Antaris, H. Dai, *Nat. Biomed. Eng.* **2017**, *1*, 0010.
- [2] Y. Ning, M. Zhu, J. L. Zhang, *Coord. Chem. Rev.* **2019**, *399*, 213028.
- [3] Z. Lei, F. Zhang, *Angew. Chemie. Int. Ed.* **2021**, *60*, 16294.
- [4] S. Wang, B. Li, F. Zhang, *ACS Cent. Sci.* **2020**, *6*, 1302.
- [5] S. Kurbegovic, K. Juhl, H. Chen, C. Qu, B. Ding, J. M. Leth, K. T. Drzewiecki, A. Kjaer, Z. Cheng, *Bioconjug. Chem.* **2018**, *29*, 3833.
- [6] S. Zhu, R. Tian, A. L. Antaris, X. Chen, H. Dai, *Adv. Mater.* **2019**, *31*, 1900321.
- [7] J. O. Escobedo, O. Rusin, S. Lim, R. M. Strongin, *Curr. Opin. Chem. Biol.* **2010**, *14*, 64.
- [8] A. G. Cosby, K. E. Martin, E. Boros, in *Modern Applications of Lanthanide Luminescence*, (Ed: A. de Bettencourt-Dias), Springer, **2021**.
- [9] M. C. Heffern, L. M. Matosziuk, T. J. Meade, *Chem. Rev.* **2014**, *114*, 4496.
- [10] J. C. G. Bünzli, C. Piguet, *Chem. Soc. Rev.* **2005**, *34*, 1048.
- [11] W. S. Lo, H. Li, G. L. Law, W. T. Wong, K. L. Wong, *J. Lumin.* **2016**, *169*, 549.
- [12] Y. Li, X. Li, Z. Xue, M. Jiang, S. Zeng, J. Hao, *Biomaterials* **2018**, *169*, 35.
- [13] M. Cieslikiewicz-Bouet, S. V. Eliseeva, V. Aucagne, A. F. Delmas, I. Gillaizeau, S. Petoud, *RSC Adv.* **2019**, *9*, 1747.
- [14] J. F. Wyart, A. Meftah, A. Bachelier, J. Sinzelle, W. Ü. L. Tchang-Brillet, N. Champion, N. Spector, J. Sugar, *J. Phys. B At. Mol. Opt. Phys.* **2006**, *39*, L77.
- [15] D. Stowiński, M. Świerczyńska, J. Romański, R. Podsiadły, *Molecules* **2022**, *27*, 8305.
- [16] C. Jiang, H. Huang, X. Kang, L. Yang, Z. Xi, H. Sun, M. D. Pluth, L. Yi, *Chem. Soc. Rev.* **2021**, *50*, 7436.
- [17] F. de Moliner, Z. Konieczna, L. Mendive-Tapia, R. S. Saleeb, K. Morris, J. A. Gonzalez-Vera, T. Kaizuka, S. G. N. Grant, M. H. Horrocks, M. Vendrell, *Angew. Chemie – Int. Ed.* **2023**, *62*, e202216231.
- [18] L. Mei, S. He, L. Zhang, K. Xu, W. Zhong, *Org. Biomol. Chem.* **2019**, *17*, 939.
- [19] M. Isaac, L. Raibaut, C. Cepeda, A. Roux, D. Boturyn, S. V. Eliseeva, S. Petoud, O. Sénèque, *Chem. – A Eur. J.* **2017**, *23*, 10992.
- [20] H. K. Kong, F. L. Chadbourne, G. L. Law, H. Li, H. L. Tam, S. L. Cobb, C. K. Lau, C. S. Lee, K. L. Wong, *Chem. Commun.* **2011**, *47*, 8052.
- [21] K. L. Gempf, S. J. Butler, A. M. Funk, D. Parker, *Chem. Commun.* **2013**, *49*, 9104.
- [22] Y. Zhang, X. Ma, H. F. Chau, W. Thor, L. Jiang, S. Zha, W. Y. Fok, H. N. Mak, J. Zhang, J. Cai, C. F. Ng, H. Li, D. Parker, L. Li, G. L. Law, K. L. Wong, *ACS Appl. Nano Mater.* **2021**, *4*, 271.
- [23] M. Starck, J. D. Fradgley, S. Di Vita, J. A. Mosely, R. Pal, D. Parker, *Bioconjug. Chem.* **2020**, *31*, 229.
- [24] H. F. Chau, Y. Wu, W. Y. Fok, W. Thor, W. C. S. Cho, P. Ma, J. Lin, N. K. Mak, J. C. G. Bünzli, L. Jiang, N. J. Long, H. L. Lung, K. L. Wong, *JACS Au* **2021**, *1*, 1034.
- [25] A. Tirla, P. Rivera-Fuentes, *Biochemistry* **2019**, *58*, 1184.
- [26] G. A. Johnson, N. Muthukrishnan, J. P. Pellois, *Bioconjug. Chem.* **2013**, *24*, 114.
- [27] Y. Wu, H. F. Chau, Y. H. Yeung, W. Thor, H. Y. Kai, W. L. Chan, K. L. Wong, *Angew. Chemie. Int. Ed.* **2022**, *61*, e202207532.
- [28] Y. Wu, H. F. Chau, H. Y. Kai, W. S. Tam, Y. H. Yeung, W. Thor, T. L. Cheung, C. Xie, J. X. Zhang, K. L. Wong, *Chem. A Eur. J.* **2023**, *29*, e202203623.
- [29] R. Varshney, P. P. Hazari, J. K. Uppal, S. Pal, R. Stromberg, M. Allard, A. K. Mishra, *Cancer Biol. Ther.* **2011**, *11*, 893.
- [30] K. L. Wong, J. C. G. Bünzli, P. A. Tanner, *J. Lumin.* **2020**, *224*, 117256.
- [31] S. E. Braslavsky, *Pure Appl. Chem.* **2007**, *79*, 293.
- [32] Y. Wu, W. S. Tam, H. F. Chau, S. Kaur, W. Thor, W. S. Aik, W. L. Chan, M. Zweckstetter, K. L. Wong, *Chem. Sci.* **2020**, *11*, 11266.
- [33] L. Jiang, H. L. Lung, T. Huang, R. Lan, S. Zha, L. S. Chan, W. Thor, T. H. Tsoi, H. F. Chau, C. Boreström, S. L. Cobb, S. W. Tsao, Z. X. Bian, G. L. Law, W. T. Wong, W. C. S. Tai, W. Y. Chau, Y. Du, L. H. X. Tang, A. K. S. Chiang, J. M. Middeldorp, K. W. Lo, N. K. Mak, N. J. Long, K. L. Wong, *Proc. Natl. Acad. Sci. U.S.A.* **2019**, *116*, 26614.
- [34] L. Jiang, R. Lan, T. Huang, C. F. Chan, H. Li, S. Lear, J. Zong, W. Y. T. Wong, M. Muk-Lan Lee, B. Dow Chan, W. L. Chan, W. S. Lo, N. K. Mak, M. Li Lung, H. Lok Lung, S. Wah Tsao, G. S. Taylor, Z. X. Bian, W. C. S. Tai, G. L. Law, W. Y. T. Wong, S. L. Cobb, K. L. Wong, *Nat. Biomed. Eng.* **2017**, *1*, 0042.